Mapping the Qademah Fault with Traveltime, Surface-wave, and Resistivity Tomograms

Sherif M. Hanafy King Abdullah University of Science and Technology (KAUST), Thuwal, Saudi Arabia*

Summary

Traveltime, surface-wave, and resistivity tomograms are used to track the buried Qademah fault located near King Abdullah Economic City (KAEC), Saudi Arabia. The fault location is confirmed by the 1) resistivity tomogram obtained from an electrical resistivity experiment, 2) the refraction traveltime tomogram, 3) the reflection image computed from 2D seismic data set recorded at the northern part of the fault, and 4) the surface-wave tomogram.

Introduction

The western side of the Kingdom of Saudi Arabia (KSA) is one of the fastest growing parts of the country, where a new city (King Abdullah Economic City (KAEC)) and a new university (King Abdullah University of Science and Technology (KAUST)) were established a few years ago. The population of KAEC is expected to be more than a million people by 2040 and the city will have one of the largest ports in the Red Sea.

Due to its expected growth, it is important to assess KAEC's earthquake hazard and proper building codes. For a complete seismic hazard assessment, paleoseismologists need to dig trenches across known faults and date the colluvial wedges to find the size and recurrence intervals of past earthquakes (McCalpin, 1996). However, paleoseismologists need to first know the locations of the faults, especially if these faults are buried. If a large earthquake (magnitude 6.0 or larger) were to occur along a near-surface hidden fault then this will likely destroy almost any man-made structure above the fault. Hence, the area above an active fault should be free of any buildings, especially hospitals, schools, and residential housing.

In this paper I present the results of using geophysical methods to track a hidden fault that intersects the King Abdullah Economic City (KAEC) in Saudi Arabia. This fault is known as Qademah Fault, and is shown on the geologic maps as an inferred fault (Roobol and Kadi, 2008), where surface geology suggests that a hidden fault runs in a north-south direction (Figure 1a). However, the exact location of the fault and its starting and ending points are not well-known. Hanafy (2012) used seismic refraction traveltime tomography, reflection, and resistivity to locate the Qademah fault around the northern part of the KAEC. In this paper, we track the fault to the southern end of KAEC using a variety of geophysical methods.

Study Area and Geological Setting

The study area in this paper is located along the western coast of KSA (Figure 1a) and is characterized by a listric normal fault system (Roobol and Kadi, 2008) located on 40 km wide coastal gravel plain. The faults are very poorly exposed as they cut unconsolidated Tertiary and Cenozoic sediments of the coastal plain, the fault scarps are eroded and typically represented by low-gravel banks.

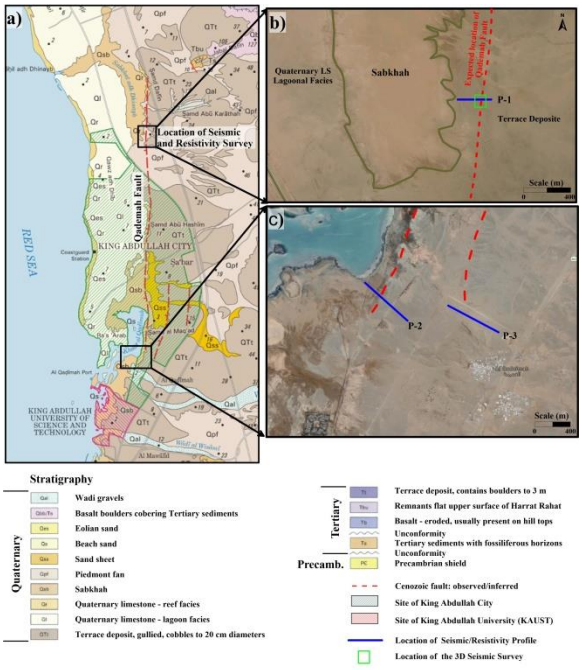

Figure 1: a) The surface geology map shows the location of the Qademah fault, after Roobol and Kadi (2008). b) and c) The north and south locations of the seismic and resistivity surveys.

In general, the Red Sea coastal plain faults are poorly exposed due to the unconsolidated nature of the coast plain sediments; however, the Qademah fault has been traced using surface geological evidence along a north-south distance of 25 km (Figure 1a). It is believed to be a normal rotational fault resulting from the opening of the Red Sea. The tilting of the sea-facing block has allowed a shallow lagoon (Figures 1a and 1c) to form along the fault scarp and also flooded the top of the down-dropped block (Figures 1a and 1b).

DOI http://dx.doi.org/10.1190/segam2015-5886064.1

Numerical Results

Three different locations are selected along the expected location of the Qademah fault. The first one is located at the northern end of the fault, where seismic and resistivity measurements are collected. The second site is located at the southern end of the fault, between KAEC and KAUST, where we only recorded seismic data.

Northern Site (P-1)

The northern site is bounded by Terrace deposits at the eastern side and a Sabkhah at the western side (Figure 1b).

a. Resistivity Tomogram

For the resistivity data, we used 64 electrodes with a 5 m electrode spacing and a Wenner-Schlumberger array configuration. The Syscal R2 instrument is used for the data collection and only data with a standard division less than 5% is accepted.

The apparent resistivity values are shown on Figure 2a. The Res2DInv software is used to invert the collected data and generate the electric resistivity tomograms (ERT) shown on Figure 2b. Five different units are shown on the ERT.

(i) **Terrace deposits.** Shown at the eastern end of the profile and characterized by resistivity values ranging between 400 and 600 Ohm.m.

(ii) **Sabkhah deposit.** This is the upper-most layer at the central and western parts of the profile and characterized by very low resistivity values (20 – 50 Ohm.m) due to the high gypsum/salt content.

(iii) **Fan deposits.** This layer underlays the Sabkhah deposits and has resistivity values ranging between 400 and 500 Ohm.m. It is composed of fine-grained loose sediments.

(iv) **Quaternary limestone.** It has resistivity values ranging between 1000 and 2000 Ohm.m and has a depth of 8 meters from the ground surface, except at the eastern part of the tomogram where it reaches 12 meters.

(v) **Interpreted colluvial wedge.** This is a local resistivity anomaly that appears between offsets of 209 and 252 m and depths from 5 to 23 m from ground surface. This low-resistivity anomaly (1 and 10 Ohm.m) is interpreted as the colluvial wedge associated with the Qademah normal fault, and is presumed to be composed of loose sediments, which accumulate saline water and reduce the resistivity values of the anomaly.

b. Seismic Refraction Tomogram

2D seismic data, labeled as P-1 in Figure 1b, are recorded at the northern site. The acquisition parameters are listed in Table 1. The picked traveltimes are inverted using traveltime tomography to generate the velocity tomogram (Nemeth et al., 1997). The final tomogram after 32 iterations is shown in Figure 3. In this figure we interpret 4 different units:

(i) **Terrace deposits.** It is characterized by low-seismic velocity values less than 600 m/s.

(ii) **Fan deposits.** The seismic velocities in this layer range between 800 and 1500 m/s and the layer thickness is about 9 meters.

(iii) **Quaternary limestone.** This layer starts at a depth of 9 meters from the ground surface, except at the eastern part of the tomogram where the depth to the top of this layer increases to about 14 meters. The seismic velocities in this layer range between 2000 and 3000 m/s and extend to the bottom of the tomogram.

(iv) **Interpreted colluvial wedge.** This low-velocity zone (LVZ) represents the colluvial wedge (1700 – 1800 m/s at X = 206 – 248 m) associated with the Qademah fault, and is mainly composed of loose sediments.

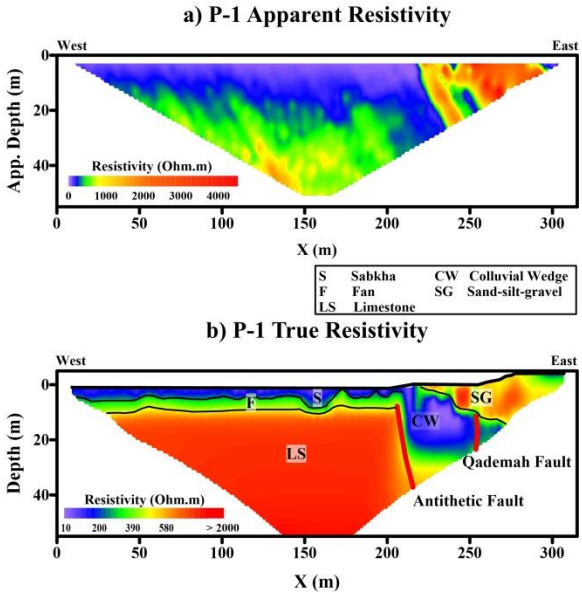

Figure 2: a) The apparent resistivity tomogram. b) The inverted electric resistivity tomogram of profile P-1 in Figure 1b shows the location of the low-resistivity colluvial wedge anomaly associated with the Qademah fault.

In the ERT both the Sabkhah and Fan deposits correspond to the upper most layer in the traveltime tomogram. In the ERT these layers can be separated due to the different fluid content in each one.

The same seismic data set is used to create the reflection stacked section (Baker, 1999) shown in Figure 3b. The Qademah fault is also seen on the reflection stacked section between offsets 227 and 249 m, which is consistent with the interpretation of the traveltime tomogram. The fault can be seen at the discontinuities of the reflectors at offset = 232 m and time = 73 ms, offset = 235 m and time = 117 ms, and offset = 238 m and time = 138 ms.

DOI http://dx.doi.org/10.1190/segam2015-5886064.1

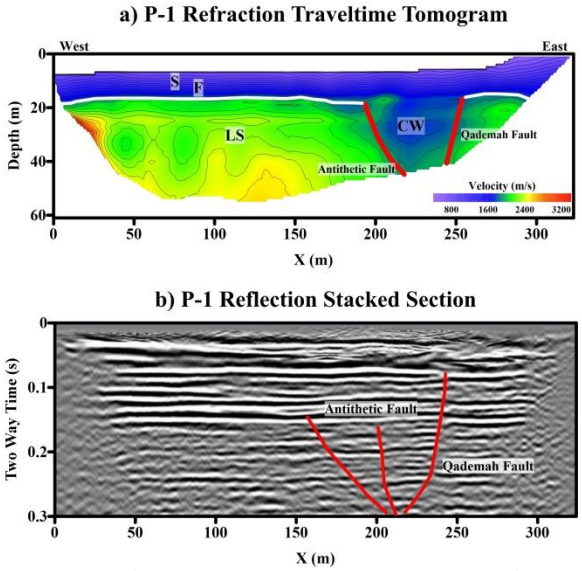

Figure 3: Profile P-1 shown in Figure 1b. a) The refraction traveltime tomogram shows the low-velocity zone (LVZ) associated with Qademah fault. b) The reflection stacked section, where the Qademah fault is shown as a discontinuity in the reflections.

Table 1: The acquisition parameters of the recorded seismic data at the northern and southern parts of Qademah Fault. The reciprocity condition is defined as the traveltime from a shot at location A to a receiver at location B should equal the traveltime from shot at location B to a receiver at location A. If a reciprocal pair of traveltimes disagrees within a specified tolerance, then both traveltimes are rejected (Sheriff, 2002).

Parameter	*Profile 1*	*Profile 2*	*Profile 3*
Location	North	South	South
No. of Shots	109	120	120
Shot Interval	3 m	5 m	5 m
No. of Receivers	109	240	120
Receiver Interval	3 m	2.5 m	5 m
Receiver Type	40-Hz	40-Hz	40-Hz
Source Type	8 kg Sledgehammer	100 kg weight drop	40 kg weight drop
Profile Length	324 m	595	595 m
Reciprocity tolerance	4 ms	4 ms	4 ms
No. of picks after reciprocity	11039	21419	13932

c. S-velocity Tomogram

A small 3D seismic data set is collected at the northern part of the Qademah fault at the same location of P-1 (Figure 1b). The data set has 12 lines each line has 24 receivers with crossline interval of 10 m and inline interval of 5 m. One shot is fired at each receiver location. This 3D seismic data set is used to find the S-velocity from the surface waves. The S-velocity estimated from the surface waves corresponds to the average S-velocity to a depth of about one wavelength (λ), where $\lambda = \frac{v}{f}$. Here, v is the S-velocity and f is the peak frequency of the surface waves (Socco and Strobbia, 2004). To find the S-velocity at different depths we apply a narrow bandpass filter to the data and find the depth of penetration associated with the peak frequency after the application of a 5-30 Hz bandpass filter. The S-wave phase velocity tomogram is shown in Figure 4, and the location of the Qademah fault is shown at the eastern side of the tomogram at an offset = 90 m. Another possible fault runs in a North-South direction and parallel to the Qademah fault at offset = 50 m as shown by the dashed line on the tomogram. The interpreted colluvial wedge due to the Qademah fault is shown as a low-velocity anomaly located between the two faults, while the low-velocity anomaly at the western side of the tomogram corresponds to the Sabkhah deposits (Figure 1a and 1b).

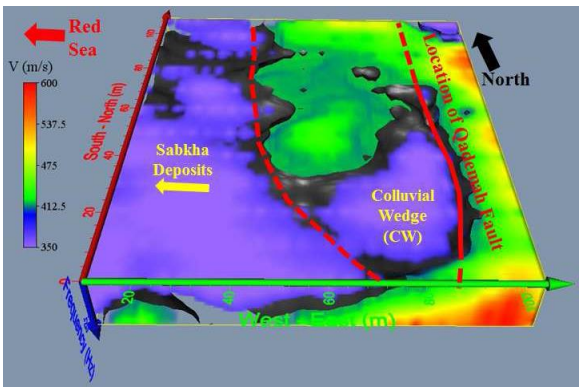

Figure 4: The S-wave phase velocity shown in a 3D block. The input data are taken from the 12 recording lines where the surface waves are used to find the phase velocity along each line. The location of the Qademah fault is shown as the solid red line, the dashed red line could be the other fault shown on the resistivity and 2D seismic images.

Southern Sites (P-2 and P-3)

Two seismic profiles (P-2 and P-3, Figure 1c) are collected at the southern part of the Qademah Fault. The acquisition parameters of both profiles are listed in table (1). The first arrival traveltimes of the shot gathers are picked, and then the traveltimes that passed the reciprocity test are inverted to generate the traveltime tomograms shown in Figures 5 and 6 for P-2 and P-3, respectively.

DOI http://dx.doi.org/10.1190/segam2015-5886064.1

In Figure 5a, a LVZ is shown between offsets X = 180 m and X = 284 m with depth ranging between 22 and 37 m from ground surface. This LVZ could be the colluvial wedge associated with the Qademah fault. The large size of the anomaly suggests that, it could be composed of more than one colluvial wedge, but due to the limitations of traveltime tomography they are smeared together and shown as one large LVZ. Figure 5b shows the common offset gather (COG) with source-receiver offset = 50 m of the collected seismic data. The surface waves show an increase in travel time between offsets 100 m and 300 m, which supports the existence of the LVZ shown in the traveltime tomogram (Figure 5a).

Figure 6a shows the traveltime tomogram of profile (P-3). A LVZ is shown between offsets X = 260 m and X = 416 m with over the depth ranging between 27 m and 64 m. The LVZ is associated with a secondary fault shown on the geological map (Figure 1a and 1c). This secondary fault is located to the east of the Qademah fault. Figure 6b shows the COG with source-offset = 40 m. The surface waves show an increase in travel time between offsets 250 and 320 m, which corresponds to the LVZ shown on the traveltime tomogram. However the size of the LVZ on the traveltime tomogram is bigger than that on the COG.

In the future, we will migrate the reflections and record a resistivity profile to refine the accuracy of our interpretation.

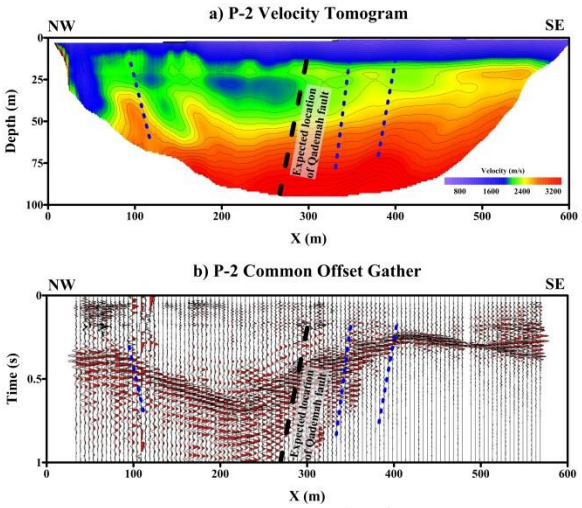

Figure 5: a) The traveltime tomogram of Profile (P-2). b) The common offset gather (COG) of profile P-2 with source-receiver offset = 50 m. Black dashed line is the Qademah fault, while the blue dashed lines are interpreted faults.

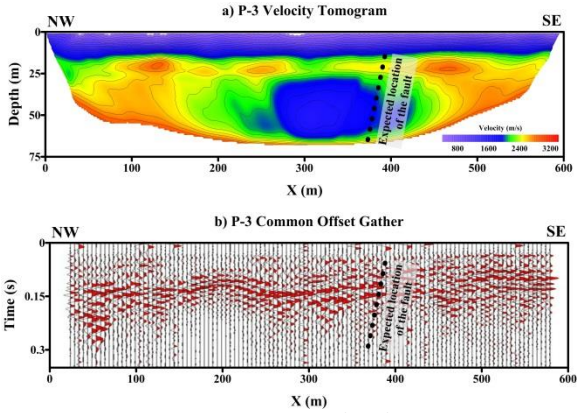

Figure 6: a) The traveltime tomogram of Profile (P-3). b) The common offset gather (COG) of profile P-3 with source-receiver offset = 40 m. Black dashed line is the expected location of the normal fault.

Conclusions

In this work we used refraction, surface-wave, and resistivity tomograms and reflection stacked sections to map the Qademah fault. Results from seismic and resistivity tomograms show low velocity/resistivity anomalies at the location of the Qademah fault. This anomaly is associated with the colluvial wedge that is formed due to the normal faulting process.

The major implication of this study is that the Qademah fault and a secondary splay exist next to both KAEC and KAUST. If this fault is active, then building codes should be designed to mitigate risk. Trenching studies should be carried out to determine the movement history of this fault.

Acknowledgements

This publication is based upon work supported by the KAUST Office of Competitive Research Funds (OCRF) under Award No.OCRF-2014-CRG3-62140387/ORS#2300

DOI http://dx.doi.org/10.1190/segam2015-5886064.1

EDITED REFERENCES

Note: This reference list is a copyedited version of the reference list submitted by the author. Reference lists for the 2015 SEG Technical Program Expanded Abstracts have been copyedited so that references provided with the online metadata for each paper will achieve a high degree of linking to cited sources that appear on the Web.

REFERENCES

Baker, G. S., 1999, Processing near-surface seismic-reflection data: A primer: SEG, http://dx.doi.org/10.1190/1.9781560802020.

Hanafy, S. M., 2012, Subsurface fault and colluvial wedge detection using resistivity, refraction tomography and seismic reflection: 74th Conference & Exhibition, EAGE, Extended Abstracts, doi:10.3997/2214-4609.20148516.

McCalpin, J. P., 1996, Paleoseismology: Academic Press.

Nemeth, T., E. Normark, and F. Qin, 1997, Dynamic smoothing in crosswell traveltime tomography: Geophysics, **62**, 168–176, http://dx.doi.org/10.1190/1.1444115.

Roobol, M. J., and K. A. Kadi, 2008, Cenozoic faulting in the Rabigh area, central-west Saudi Arabia (including the sites of King Abdullah Economic City and King Abdullah University of Science and Technology): Saudi Geological Survey Technical Report SGS-TR-2008-6, ftp://137.227.224.179/brocher/Saudi%20Arabia/Saudi%20Literature/Roobol_SGS_TR_2008_6/RoobolSGS_TR_2008_6_2008text.pdf.

Sheriff, R. E., 2002, Encyclopedic dictionary of applied geophysics, 4th ed.: SEG, http://dx.doi.org/10.1190/1.9781560802969.

Socco, L. V., and C. Strobbia, 2004, Surface-wave method for near-surface characterization: A tutorial: Near Surface Geophysics, **2**, no. 4, 165–185, http://dx.doi.org/10.3997/1873-0604.2004015.